Article

Not peer-reviewed version

Assessing the Internal Structural Integrity of *Ceroxylon* Palms Using Sonic Tomography in Tropical Montane Forests of the Peruvian Andes

Doris Gómez-Ticerán , Abel Salinas-Inga , Jehoshua Macedo-Bedoya , Marcel La Rosa-Sánchez , Fernando Camones-Gonzales , Franco Angeles-Alvarez , Marco Carbajal-Bellido , Bruno Padilla-Torres , Paola Morosini-Inga , Luis Alberto León-Bañuelos , Yakov Quinteros-Gómez *

Posted Date: 5 May 2026

doi: 10.20944/preprints202605.0217.v1

Keywords: *Ceroxylon*; forest health monitoring; sonic tomography; palm structural integrity; non-destructive palm assessment

 doi:10.20944/preprints202605.0217.v1

Article

Assessing the Internal Structural Integrity of *Ceroxylon* Palms Using Sonic Tomography in Tropical Montane Forests of the Peruvian Andes

Doris Gómez-Ticerán [1], Abel Salinas-Inga [1,2], Jehoshua Macedo-Bedoya [1,2], Marcel La Rosa-Sánchez [1,2], Fernando Camones-Gonzales [3], Franco Angeles-Alvarez [1,2], Marco Carbajal-Bellido [1,2], Bruno Padilla-Torres [2], Paola Morosini-Inga [1], Luis Alberto León-Bañuelos [4] and Yakov Quinteros-Gómez [1,2,*]

[1] Grupo de Investigación MOCA, Facultad de Ciencias Matemáticas, Universidad Nacional Mayor de San Marcos (UNMSM), Lima 15081, Peru
[2] Laboratorio de Ecología Tropical y Análisis de Datos, Facultad de Ciencias Biológicas, Universidad Nacional Mayor de San Marcos (UNMSM), Lima 15081, Peru
[3] Departamento Académico de Estadística, Universidad Nacional Mayor de San Marcos (UNMSM), Lima 15081, Peru
[4] Tecnológico Nacional de México / TES Valle de Bravo. Km. 30, Carretera Federal Monumento Valle de Bravo, San Antonio de la Laguna, 51200 Valle de Bravo, Estado de México
* Correspondence: yquinterosg@unmsm.edu.pe

Abstract

Palms of the genus *Ceroxylon* constitute a key component of Andean tropical montane forests; however, their internal structural integrity has been scarcely studied in Peru. The present study assessed the internal structural condition of natural populations within the Private Conservation Area (PCA) Bosque de Palmeras of the Taulía-Molinopampa Peasant Community using sonic tomography, a non-invasive technique for detecting cavities and decay in the stipe. A total of 64 individuals distributed across four zones with differing degrees of anthropogenic disturbance — passive recovery, reforestation, active cattle ranching, and mixed forest — were analyzed, generating 256 tomograms at four vertical levels. Results revealed high levels of structural deterioration across all zones (59.8%–67.9%), with the greatest affectation recorded in the active cattle ranching zone, and significant differences among zones (Kruskal–Wallis, $p < 0.05$). A significant positive correlation was found between diameter at breast height (DBH) and structural damage ($\varrho = 0.298$; $p = 0.0168$), whereas altitude showed no significant association ($p = 0.7462$). Structural deterioration exhibited a heterogeneous distribution both vertically and among individuals. Taken together, these findings indicate that anthropogenic activities increase structural deterioration and compromise the stability of *Ceroxylon* populations, and confirm the potential of sonic tomography as an effective tool for the monitoring and conservation of Andean palms.

Keywords: *Ceroxylon*; forest health monitoring; sonic tomography; palm structural integrity; non-destructive palm assessment

1. Introduction

In the Neotropics, palms (Arecaceae) represent one of the most diverse and ecologically significant plant groups, comprising approximately 181 genera and 2600 species [1]. These species are integral components of a wide variety of ecosystems, including tropical rainforests, palm swamps, restingas, peatlands, and palm savannas [2,3]. Their distribution and abundance are primarily determined by climatic factors such as temperature and precipitation, as well as edaphic conditions related to soil drainage and fertility [4]. These environmental variables exert a significant

 doi:10.20944/preprints202605.0217.v1

influence on palm diversity and dominance patterns, which accounts for their marked prevalence in tropical and subtropical regions [5,6].

Beyond their high diversity, palms constitute a key structural and functional component of tropical forests, particularly in the Neotropical region, where they contribute substantially to forest architecture and resource provisioning for diverse faunal assemblages [7,8]. They also play a fundamental role in the livelihoods of numerous local communities, providing food, construction materials, and other products of economic and cultural value. Among the most ecologically relevant genera are Euterpe, Mauritia, Astrocaryum, and Attalea, which are widely distributed throughout the Amazonian region, as well as Ceroxylon, which occurs at elevations above 2000 m a.s.l. All of these genera are recognized both for their ecological importance and their multiple traditional uses and potential medicinal applications [3,9,10].

Ceroxylon (Arecaceae) is a genus endemic to the tropical Andes, distributed primarily in transitional zones between high Andean and Amazonian regions [2]. This palm genus comprises 13 species distributed across six South American countries, from Venezuela to Bolivia, spanning altitudinal ranges of 800–3500 m a.s.l., with a notable presence in humid montane and cloud forests [11,12]. Peru harbors seven Ceroxylon species, two of which are endemic (C. peruvianum and C. ravenii), with records from the departments of Piura, Cajamarca, Amazonas, Ucayali, Junín, Cusco, Ayacucho, and Puno [11–13].

Morphological descriptions of the genus *Ceroxylon*, encompassing species such as *C. quindiuense*, *C. alpinum*, *C. ceriferum*, and *C. parvifrons*, consistently report the presence of a solitary, unbranched stipe that elongates progressively throughout the plant's life cycle [14–16]. This trait reflects a monopodial growth pattern that has been widely documented for the genus in recent taxonomic revisions [11]. Even in atypical cases such as *Ceroxylon ravenii*, which exhibits an acaulescent habit, the morphology remains defined by a single, unbranched, reduced axis arranged in a rosette form [12].

In South America, several *Ceroxylon* species face varying levels of threat, primarily driven by anthropogenic pressures [17,18]. A representative example is *Ceroxylon quindiuense*, a Colombian endemic classified as Endangered (EN), whose population decline is mainly attributed to the expansion of cattle ranching and agricultural encroachment [11,19,20]. Similarly, species such as *C. alpinum* and *C. ventricosum* are subject to selective extraction for wax harvesting and the collection of fronds used in religious rituals during Holy Week [11,20]. Although this practice constitutes a deeply rooted cultural tradition in Andean communities, its continuation has contributed to significant population decline [21]. In this context, it is a priority to strengthen knowledge on the population structure and health status of *Ceroxylon* populations in Peru through systematic monitoring and forest assessments, which will provide key information for defining evidence-based management and conservation strategies.

The various tools available for forest monitoring enable early detection of wildfires, pest outbreaks, land-use change-driven deforestation, and the effects of climate change on the structure and dynamics of plant communities [22,23]. Nevertheless, knowledge of the internal health of trees (the primary structural component of forests) remains limited [24]. Over the past decade, advances in remote sensing and the use of unmanned aerial vehicles (UAVs) have substantially expanded the capabilities for vegetation analysis [25], while the development of specialized models and algorithms has improved the characterization of canopy structure and dynamics [26]. However, these approaches have inherent limitations for directly and systematically assessing the internal condition of trees at the population scale [27]. Conventional methods such as increment core sampling with a Pressler borer or resistography allow examination of woody tissue condition, but involve a considerable degree of invasiveness [28]. In contrast, Sonic Tomography (ST) has emerged as a modern, non-invasive tool for assessing the internal condition of tree stems, enabling the detection of cavities, decay, and other structural defects with minimal impact on the tree [24,29].

Despite the ecological and socioeconomic relevance of palms of the genus *Ceroxylon*, available information on the internal structural condition and health status of their natural populations

 doi:10.20944/preprints202605.0217.v1

remains scarce, particularly in Peru. This knowledge gap limits understanding of the structural degradation processes that may affect long-term stability, survival, and population dynamics. In this context, the present study aimed to assess the internal structural condition of *Ceroxylon* individuals within natural populations in the Private Conservation Area (PCA) Bosque de Palmeras of the Taulía Molinopampa Peasant Community, using Sonic Tomography, a non-invasive technique for detecting cavities, decay, and other internal stem defects. The findings of this study provide relevant evidence to support monitoring, management, and conservation strategies for *Ceroxylon* in tropical montane forests of the Andes.

2. Materials and Methods

2.1. Study Sites

The study was conducted over a two-week period in August 2024 in the wax palm forests located in the community of Ocol, district of Molinopampa, province of Chachapoyas, department of Amazonas, Peru. These forests form part of the Private Conservation Area (PCA) "Bosque de Palmeras de la Comunidad Campesina Taulia-Molinopampa", established in 2012 and covering an area of 10,938 hectares [30] for a period of 40 years (Property Registration No. 02013763). The wax palm forests are distributed between 2,000 and 3,000 m a.s.l. within Andean humid montane forest ecosystems [31], characterized by cool temperatures and high atmospheric humidity — the typical habitat of palms of the genus Ceroxylon [32]. Mean annual temperature is 14.5 °C and mean annual precipitation is 1,200 mm, corresponding to the tropical montane humid forest life zone (bosque húmedo Montano Tropical, bh-MT) [33]. These populations occur in montane forests characterized by the headwaters of hydrographic basins and micro-watersheds [34], where they perform critical functions in water regulation and habitat provision [13].

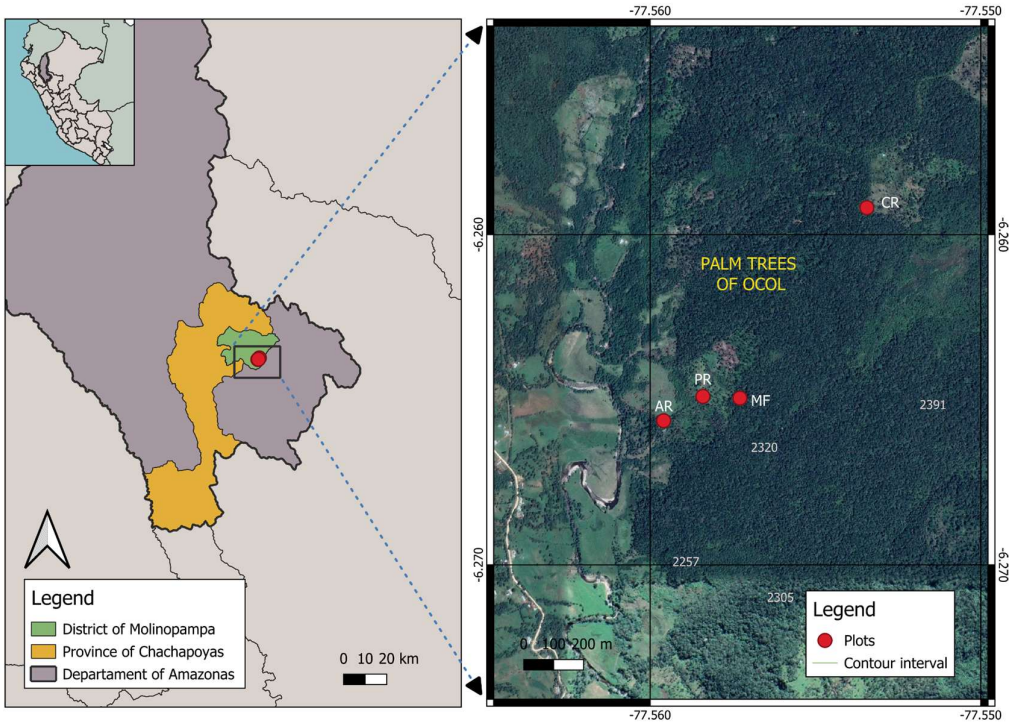

Figure 1. Location of the study area and distribution of the four evaluation zones categorized according to their history of anthropogenic disturbance: PR (passive restoration), AR (active restoration/reforestation), CR (cattle ranching), and MF (mixed forest).

 doi:10.20944/preprints202605.0217.v1

Field surveys were conducted to identify potential study zones based on the characterization of contrasting land-use histories, prioritizing areas with the highest density of adult palms. Four study zones were established: (i) Passive restoration (PR): a previously intervened and deforested area in which only adult Ceroxylon palms were left standing and which was temporarily used for cattle grazing; (ii) Active restoration/Reforestation (AR): a partially deforested area that was not used for cattle ranching and where a local reforestation program was initiated four years ago; natural regeneration is currently underway; (iii) Cattle ranching (CR): the most remote zone from the community, characterized by extensive deforestation in which only adult Ceroxylon palms were retained, and where permanent cattle presence prevents natural regeneration; (iv) Mixed forest (MF): a forest located at mid-slope elevation with a low level of anthropogenic disturbance.

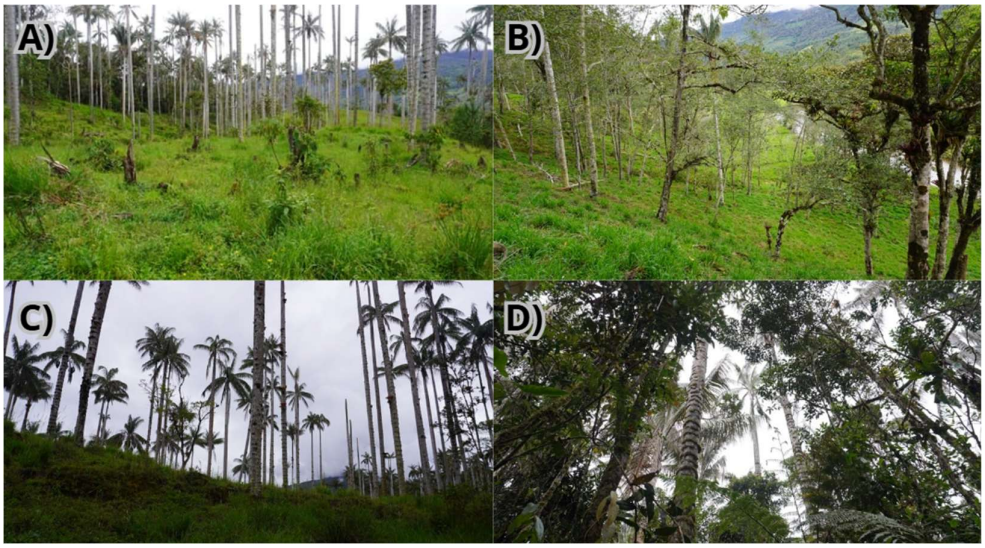

Figure 2. Schematic representation of the four study zones characterized by contrasting land-use histories and Ceroxylon palm density: A) Passive Restoration (PR): a post-grazing recovery area featuring legacy adult palms as structural remnants; B) Active Restoration (AR): a managed reforestation site under a 4-year-old enrichment program with ongoing natural regeneration; C) Cattle Ranching (CR): an anthropogenically degraded zone where continuous grazing pressure inhibits the recruitment of new woody individuals; and D) Mixed Forest (MF): a primary forest reference site at mid-slope elevation with minimal anthropogenic disturbance.

Within each of the described zones, four plots (10 × 10 m) were established, in which four individuals (DBH > 10 cm) were assessed per plot, and four tomograms were generated per individual. This sampling design yielded 64 tomograms per zone and 256 tomograms in total. Tree selection was based on the following criteria: (i) accessibility of each individual, (ii) preliminary visual assessment of the stipe showing no apparent external damage, and (iii) DBH > 10 cm.

2.2. Sonic Tomography

The internal structure of the palms was assessed using the ArborSonic 3D (AS3D) sonic tomograph, a high-resolution non-invasive technique designed to detect internal structural anomalies in trees and palms [35]. This instrument evaluates structural integrity through the propagation of stress waves, based on the relationship $V = \sqrt{(E/\varrho)}$ [36]. The AS3D measures the Time of Flight (ToF) between transducers; in healthy tissue, wave propagation is rapid and direct, whereas the presence of cavities or fungal decay increases ToF by forcing the signal to deviate or pass through low-density zones [37] Despite the complex anisotropy of palm tissue, the instrument processes a dense matrix of acoustic trajectories to map decay zones [38]. The resulting data are transformed from temporal measurements into velocity-gradient tomograms, facilitating the early detection of structural defects that are not externally visible [39].

 doi:10.20944/preprints202605.0217.v1

Figure 3. A) Field activities and configuration of the ArborSonic 3D (AS3D) sonic tomograph on palm individuals. The research team is shown conducting field measurements, and B) the installation of the instrument on the stipe, illustrating sensor placement and the measurement procedure for correct setup.

Prior to AS3D installation, a biosecurity protocol was implemented consisting of sensor disinfection with 70% ethanol and the application of a broad-spectrum insecticide, in order to minimize the risk of pathogen transfer between individuals. The technical procedure involved the installation of ten acoustic sensors and five transmitter modules distributed equidistantly around the perimeter of the stipe [40]. These devices were connected to a central control unit (laptop computer) responsible for recording and processing the acoustic data, generating color-coded tomograms that represent the spatial variation in wood density and structural integrity [37].

To characterize the vertical profile of the internal structure, measurements were taken at four standardized cross-sectional levels located at 10, 30, 50, and 70 cm above ground level. Tomogram generation was accomplished by delivering light hammer strikes to each sensor, producing acoustic waves whose transverse propagation velocity was recorded by the system [41]. Variations in wave velocity and trajectory, which are related to stem density and integrity [42], enabled the identification of irregularities associated with internal cavities or decay processes, and allowed the quantification of internal damage as a percentage of the cross-sectional area of the stipe. Decay percentages were subsequently processed using ArborSonic 3D software v5.3.162, classifying damage severity into three risk categories: low (<30%), moderate (30%–60%), and high (>60%) [43].

2.3. Data Analysis

An exploratory data analysis was conducted through graphical representation of the relationships between the independent variables (zone, plot, diameter at breast height (DBH), and altitude) and the dependent variable, mean structural damage across the four tomographic measurement levels. Box plots were used to identify trends and examine the effect of the independent variables on mean damage. This descriptive statistical approach facilitated a preliminary visual interpretation of the data as a function of zone, plot, and mean damage.

Subsequently, a more detailed statistical analysis was performed using the non-parametric Kruskal–Wallis test, which was selected given that the variable zone comprises four categories, allowing for the assessment of significant differences among the groups analyzed. Scatter plots were additionally constructed to examine the relationships between DBH, altitude, and mean damage, as well as the combined effect of zone and plot with DBH and altitude. These plots provided a comprehensive perspective on the influence of the independent variables on mean structural damage. To ensure the validity of the results, normality tests were applied to all quantitative variables in order to determine their suitability for non-parametric analyses, including Spearman's rank correlation. The combined effect of the independent variables was subsequently evaluated using a linear mixed model.

 doi:10.20944/preprints202605.0217.v1

All analyses were performed in RStudio (R version 4.3.0), using the following packages: lme4 for linear and generalized linear mixed models [44], ggplot2 v3.5.2 for data visualization [45], dplyr v1.1.4 for data manipulation [46], and lmerTest v3.1.3 for significance testing in mixed models [47].

3. Results

3.1. Tomograms and Level of Wood Decay

A total of 256 tomograms were generated across the four study zones for 64 individuals. Decay percentages ranged from minimally affected individuals (53.50%) to severely affected specimens (100.00% decay) (Table 1).

Table 1. Data from the assessment of internal structures in Ceroxylon using sonic tomography, including zone, plot number, number of trees, DBH, altitude, decay percentage for each of the four assessed levels, and their mean values.

Zone	Plot	Tree	DBH	Altitude	Layer 1	Layer 2	Layer 3	Layer 4	Average Damage
AR	1	1	34	2257	64	76	64	67	67.75
AR	1	2	35	2257	74	71	69	70	71.00
AR	1	3	33	2257	58	57	55	58	57.00
AR	1	4	35	2257	65	63	54	56	59.50
AR	2	1	41	2257	56	53	54	52	53.75
AR	2	2	30	2257	57	57	55	53	55.50
AR	2	3	35	2257	55	54	57	54	55.00
AR	2	4	32	2257	67	77	62	57	65.75
AR	3	1	35	2257	58	57	55	56	56.50
AR	3	2	39	2257	80	79	68	63	72.50
AR	3	3	35	2257	67	67	64	65	65.75
AR	3	4	34	2257	53	56	61	62	58.00
AR	4	1	32	2257	72	70	63	66	67.75
AR	4	2	40	2257	61	70	65	60	64.00
AR	4	3	39	2257	64	66	60	61	62.75
AR	4	4	39	2257	69	70	69	68	69.00
PR	1	1	38	2305	71	55	57	53	59.00
PR	1	2	39	2305	73	60	62	59	63.50
PR	1	3	30	2305	48	64	53	57	55.50
PR	1	4	37	2305	64	64	69	61	64.50
PR	2	1	56	2305	96	90	87	80	88.25
PR	2	2	28	2305	61	58	52	55	56.5
PR	2	3	46	2305	68	67	61	66	65.5
PR	2	4	34	2305	72	58	76	53	64.75
PR	3	1	41	2305	74	91	71	61	74.25

 doi:10.20944/preprints202605.0217.v1

PR	3	2	40	2305	57	55	55	54	55.25
PR	3	3	38	2305	60	55	60	58	58.25
PR	3	4	49	2305	68	62	60	57	61.75
PR	4	1	32	2305	55	52	55	52	53.50
PR	4	2	35	2305	59	66	60	55	60.00
PR	4	3	35	2305	69	69	68	70	69.00
PR	4	4	38	2305	72	78	73	76	74.75
MF	1	1	27	2320	55	54	54	59	55.50
MF	1	2	36	2320	58	54	56	58	56.50
MF	1	3	35	2320	53	53	54	59	54.75
MF	1	4	27	2320	57	58	57	58	57.50
MF	2	1	42	2320	59	58	57	56	57.50
MF	2	2	42	2320	53	57	56	56	55.50
MF	2	3	30	2320	58	56	56	56	56.50
MF	2	4	26	2320	100	100	100	100	100.00
MF	3	1	35	2320	58	56	54	55	55.75
MF	3	2	37	2320	57	56	56	53	55.50
MF	3	3	26	2320	51	55	54	58	54.50
MF	3	4	31	2320	55	59	54	57	56.25
MF	4	1	36	2320	71	58	57	53	59.75
MF	4	2	42	2320	55	56	53	57	55.25
MF	4	3	45	2320	72	63	71	63	67.25
MF	4	4	35	2320	57	66	56	54	58.25
CR	1	1	30	2391	64	57	53	59	58.25
CR	1	2	31	2391	75	80	67	75	74.25
CR	1	3	37	2391	75	73	78	85	77.75
CR	1	4	40	2391	80	77	75	78	77.50
CR	2	1	44	2391	59	59	60	56	58.50
CR	2	2	35	2391	53	56	54	52	53.75
CR	2	3	48	2391	79	61	61	61	65.50
CR	2	4	45	2391	93	85	80	74	83.00
CR	3	1	46	2391	72	62	54	54	60.50
CR	3	2	47	2391	73	58	60	60	62.75
CR	3	3	43	2391	73	68	63	56	65
CR	3	4	35	2391	69	69	59	55	63
CR	4	1	39	2391	71	60	52	63	61.50
CR	4	2	45	2391	100	100	100	97	99.25
CR	4	3	38	2391	52	55	59	58	56.00
CR	4	4	38	2391	81	62	70	69	70.50

 doi:10.20944/preprints202605.0217.v1

The PR site exhibited a mean deterioration of 64.02%. The most affected individual displayed a distinctive vertical decay pattern, with the basal level (Level 1) showing minimal damage compared to Level 2, where sensors 3, 4, 5, and 6 detected affected areas (96% decay). Level 3 showed localized damage at sensor 7, while Level 4 presented affected zones at sensor 9. In contrast, the least affected individual at this site showed relatively uniform deterioration across all stem levels, with Levels 2 and 4 being the best-preserved sections, recording 52% decay.

The AR site presented a mean deterioration of 62.59%. The most affected individual showed damage concentrated in the basal level, particularly at sensors 1 and 5. This pattern persisted in Level 2, where sensors 1 and 5 again exhibited the greatest deterioration (77% decay). Level 3 displayed a more uniform and less affected structure across all sensors, while Level 4 showed the lowest damage levels (52% decay). The least affected individual at this site exhibited a relatively homogeneous deterioration distribution across all levels, with Level 1 showing the greatest deterioration compared to the remaining levels (56% decay).

The CR site showed the highest mean deterioration (67.94%) among all sites. The most affected individual exhibited extensive damage in Level 1, with sensors 2, 3, 4, 6, 7, 8, 9, and 10 detecting affected areas. Level 2 at this site showed critically compromised areas (100% decay), with all monitored sensors affected throughout this section. Level 3 showed a marked improvement, with damage localized exclusively at sensor 8, while Level 4 showed improved structural integrity, yet still recorded a high decay percentage (97% decay). The least affected individual showed localized decay in Level 1 (53% decay) at sensors 2 and 9. Level 2 exhibited improved internal structure with no damage detected by the sensors (56% decay). Level 3 maintained minimal deterioration, with damage confined to sensor 9, while Level 4 showed affected areas only at sensor 2, with all remaining sensors indicating reduced decay.

The MF site recorded the lowest mean deterioration (59.8%) among all zones. The most affected individual presented extensive damage in the basal level, with sensors 3, 4, 5, 6, 7, and 8 detecting affected zones. Level 2 showed reduced deterioration relative to the basal section, while Levels 3 and 4 maintained relatively stable conditions with minimal damage detected by the sensors throughout the internal structure. The least affected individual exhibited localized deterioration patterns: Level 1 showed damage only at sensor 5 (51% decay), Level 2 at sensor 9 with lesser deterioration (55% decay), Level 3 at sensors 2 and 6 (54% decay), and Level 4 at sensors 5 and 7 (58% decay).

 doi:10.20944/preprints202605.0217.v1

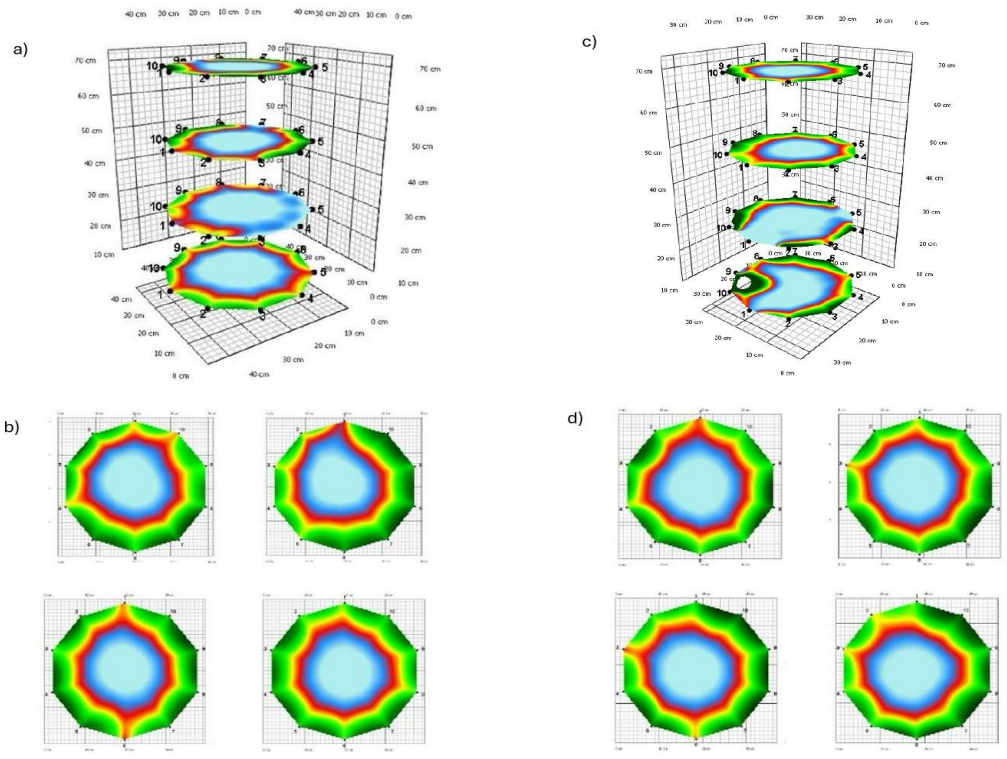

Figure 4. Comparative tomographic analysis of Ceroxylon spp. in Study Sites 1 and 2: (a, c) cross-sections showing maximum internal decay in Z1 and Z2, respectively; (b, d) cross-sections showing minimum internal decay in Z1 and Z2, respectively.

 doi:10.20944/preprints202605.0217.v1

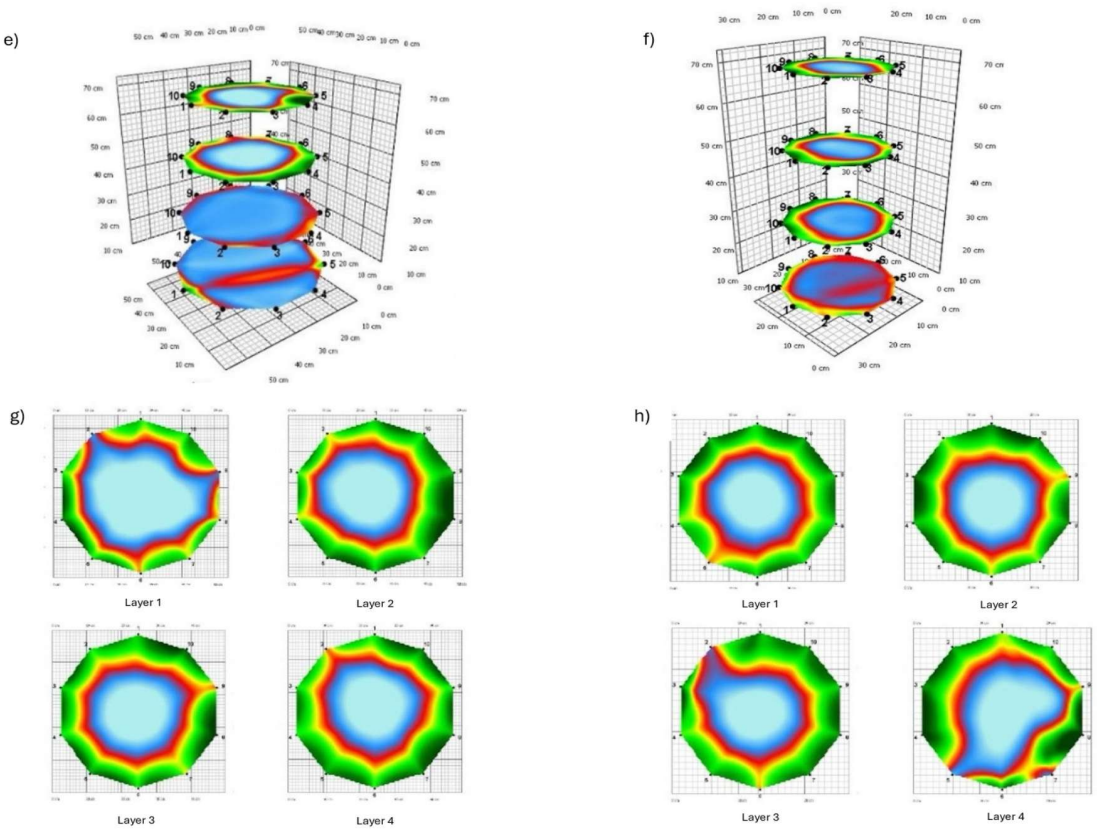

Figure 5. Comparative tomographic analysis of Ceroxylon spp. in Study Sites 3 and 4: (a, c) cross-sections showing maximum internal decay in Z3 and Z4, respectively; (b, d) cross-sections showing minimum internal decay in Z3 and Z4, respectively.

3.2. Analysis Results

Normality test results indicated that zones AR ($p = 0.267$), PR ($p = 0.051$), and CR ($p = 0.059$) did not reject the null hypothesis of normality, whereas zone MF ($p = 0.0000010$) did, evidencing a non-normal distribution in that area. Given this heterogeneity in data distribution, the non-parametric Kruskal–Wallis test was applied to compare mean damage among zones. The result ($\chi^2 = 9.975$, $df = 3$, $p = 0.019$) indicated statistically significant differences, implying that at least two zones exhibit distinct levels of structural damage. This finding supports the graphical evidence of inter-zonal variability and confirms that the impact on palm individuals is not homogeneous across the forest.

Following the significant Kruskal–Wallis result ($\chi^2 = 9.98$, $df = 3$, $p = 0.019$), a post-hoc Dunn test with Bonferroni correction was conducted, identifying a single statistically significant pairwise difference between the mixed forest (MF) and cattle ranching (CR) zones ($Z = -3.06$, $padj = 0.013$). In contrast, comparisons between MF and active restoration (AR) ($Z = -2.01$, $padj = 0.267$) and between MF and passive restoration (PR) ($Z = -2.13$, $padj = 0.200$) did not reach statistical significance. The remaining pairwise comparisons (CR–AR, CR–PR, and AR–PR) likewise showed no significant differences, with $padj > 0.05$ in all cases. These findings confirm that MF is distinguished as the zone with the lowest relative structural damage, while CR concentrates the highest and most variable damage levels among wax palm individuals. From a conservation standpoint, MF may be considered a reference area with lower anthropogenic impact, whereas CR requires priority attention given its greater severity and dispersion in damage levels.

Normality was assessed using the Shapiro–Wilk test. Results indicated that DBH conformed to a normal distribution ($W = 0.975$; $p = 0.219$), whereas both altitude ($W = 0.832$; $p < 0.001$) and mean structural damage ($W = 0.810$; $p < 0.001$) showed significant departures from normality. Accordingly,

 doi:10.20944/preprints202605.0217.v1

Spearman's rank correlation was used for association analyses. A statistically significant positive correlation was found between DBH and mean structural damage in Ceroxylon spp. ($\varrho = 0.298$; S = 30,666; p = 0.017), suggesting that larger individuals exhibit greater susceptibility to, or cumulative accumulation of, structural damage. In contrast, altitude showed no significant association with the phytosanitary condition of the palms ($\varrho = 0.041$; S = 41,878; p = 0.746). Collectively, these findings underscore the importance of DBH as a predictor of structural damage in wax palms, while altitude appears to exert only a marginal and inconsistent influence. These results reinforce the need to incorporate individual structural characteristics as a priority criterion in the design of conservation and adaptive management strategies.

Figure 6 illustrates the distribution of mean structural damage in wax palms (Ceroxylon spp.) across the four forest zones of Molinopampa: AR, PR, MF, and CR. Zones AR and PR exhibited similar levels of damage, with median values close to 65% and intermediate variability, reflected in the presence of outliers exceeding 90%. Zone MF was distinguished by the lowest median (approximately 55%) and reduced dispersion, suggesting a relatively more homogeneous and less critical condition. In contrast, zone CR displayed the greatest distributional range, with extreme values reaching 100%, evidencing localized foci of severe deterioration. Although MF appears as the least impacted zone, the presence of an outlier at 100% confirms that even in areas with lower mean damage, highly affected individuals can occur. This comparative characterization enables the identification of priority zones for conservation and management actions, particularly in CR, where high variability and critical cases demand immediate attention.

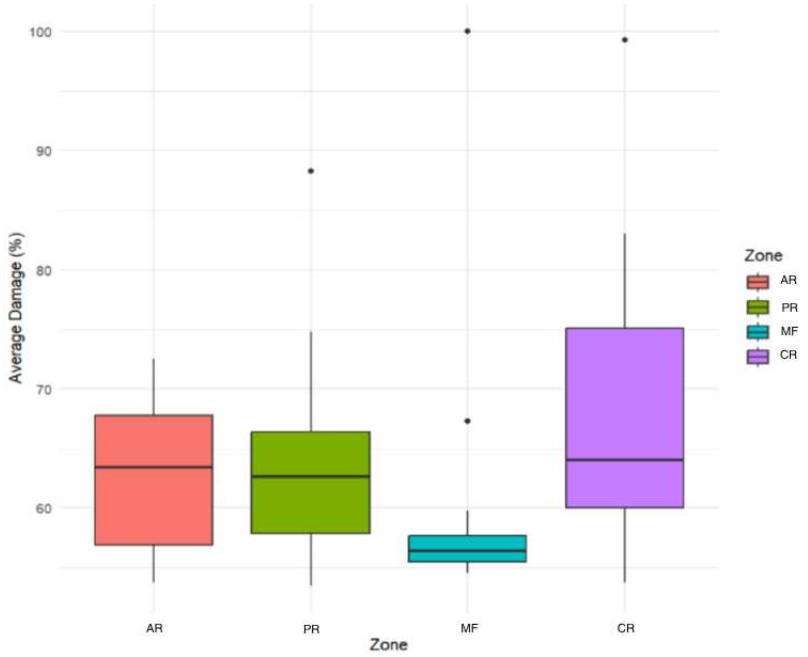

Figure 6. Damage Distribution in Wax Palms (*Ceroxylon* spp.) by Zone.

Figure 7 depicts the distribution of mean structural damage (%) in wax palms (Ceroxylon spp.) by plot within each forest zone of Molinopampa, Amazonas. Zones AR and PR showed similar damage medians, close to 65%, although with internal variability among plots and the presence of outliers exceeding 90%, suggesting localized pressures. Zone CR was distinguished by its greater dispersion, particularly in Plot 4, where extreme values approaching 100% were recorded, evidencing critical damage hotspots. In contrast, zone MF maintained the lowest mean damage level (approximately 55%), with a more homogeneous distribution among plots, though it also presented an outlier at 100%, confirming that even in less impacted areas, highly affected individuals occur.

 doi:10.20944/preprints202605.0217.v1

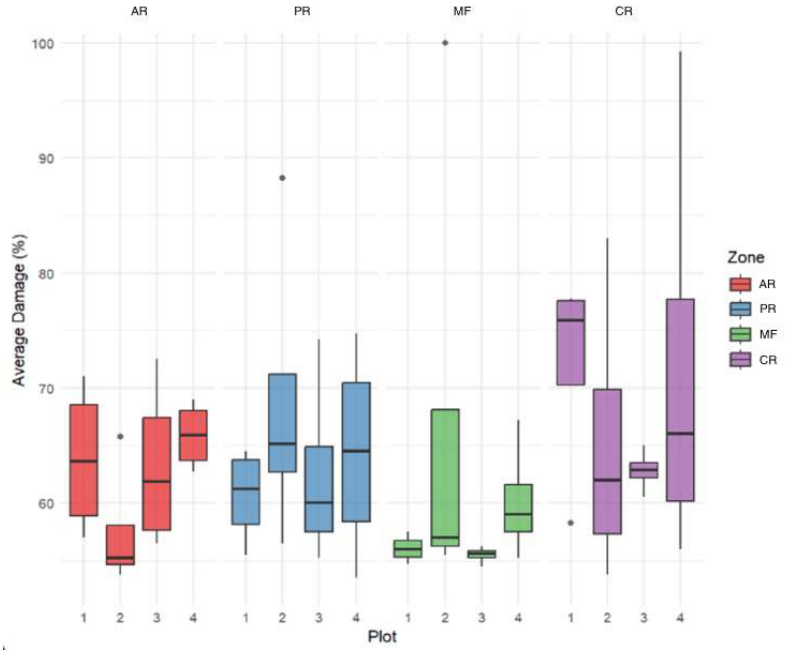

Figure 7. Effect of Zone and Plot on Average Damage (%).

This comparative analysis enables the identification of damage patterns at both plot and zone scales, providing key information for focusing conservation actions and designing adaptive management strategies. In particular, the variability observed in CR and the outliers in AR and PR suggest the need for targeted interventions in critical plots, while MF may be considered a reference area for evaluating less severe baseline conditions.

Figure 8 presents the distribution of percentage structural damage in wax palms (Ceroxylon spp.) in the Molinopampa forest, Amazonas, assessed by zone (AR, PR, MF, and CR), plot (Plots 1–4), and structural layer (Layers 1–4). Each panel represents damage at a specific cross-sectional level, from the base (Layer 1) to the upper section (Layer 4), enabling analysis of vertical damage patterns in relation to spatial location.

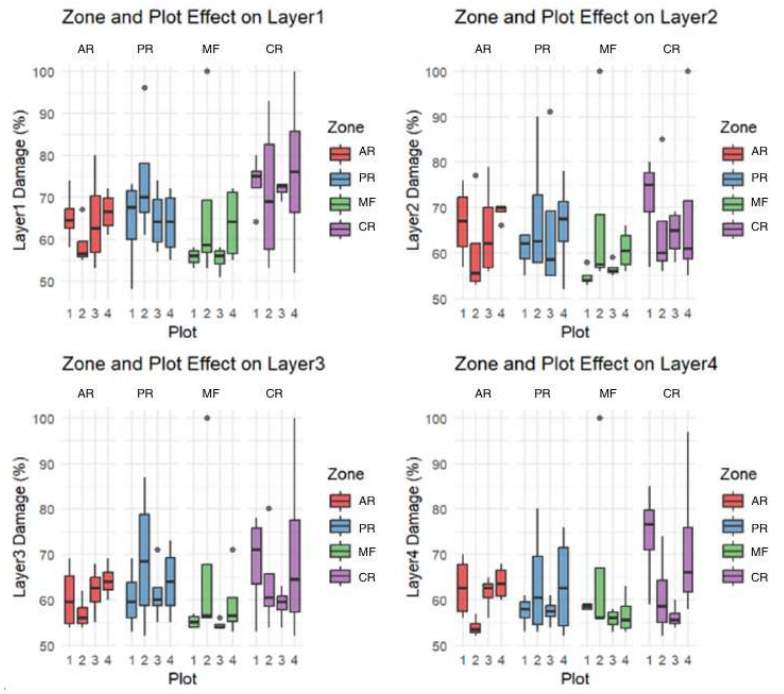

 doi:10.20944/preprints202605.0217.v1

Figure 8. Zone and Plot Effect on Layer 1, 2, 3 y 4.

Zones AR and PR exhibited similar damage medians (approximately 65%) across all layers, with intermediate inter-plot variability and the presence of outliers exceeding 90%, potentially associated with localized pressures at specific structural levels. Zone CR was notable for its greater dispersion across all layers, particularly in Plot 4, where extreme values approaching 100% were recorded, indicating critical foci of structural deterioration. In contrast, zone MF maintained the lowest mean damage level (approximately 55%) across all layers, with a more homogeneous inter-plot distribution, although outliers at 100% were also present, confirming that even in less impacted areas, highly affected individuals exist.

This analysis allows the identification of both vertical and spatial damage patterns, providing key information for designing differentiated conservation strategies by zone, plot, and structural layer. In particular, the high variability in CR and the outliers in AR and PR underscore the need for targeted interventions in critical plots, while MF may serve as a reference area for assessing less severe conditions.

Figure 9 illustrates the relationship between mean structural damage (%) in wax palms (Ceroxylon spp.) and two key ecological variables — diameter at breast height (DBH, cm) and altitude (m a.s.l.) — in the Molinopampa forest, Amazonas, Peru.

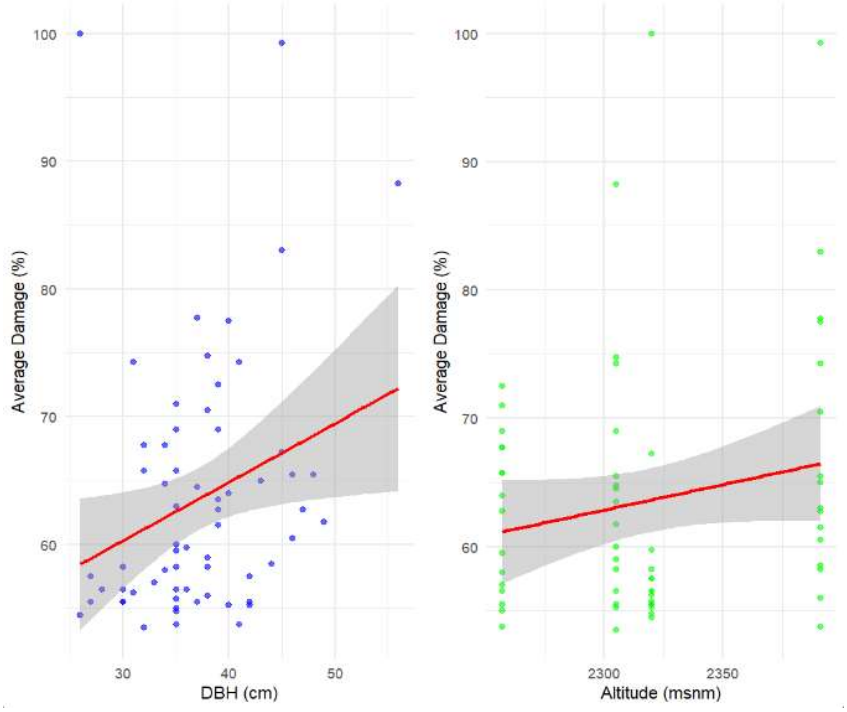

Figure 9. Relationship between DBH, Altitude and Average Damage.

The left panel reveals a positive correlation between DBH and mean damage, indicating that larger individuals tend to exhibit higher levels of structural deterioration. This trend may be explained by the greater visibility and accessibility of palms with larger diameters, which may render them more vulnerable to external pressures such as pest infestation, selective extraction, or cattle impact. The right panel shows a positive, though weaker, correlation between altitude and mean damage, suggesting that palms located at higher elevations tend to record slightly greater deterioration, possibly associated with specific microclimatic conditions or the presence of environmental stressors at higher altitudes.

 doi:10.20944/preprints202605.0217.v1

Taken together, both patterns reinforce the importance of incorporating structural variables (such as individual size) and topographic variables (such as altitude) into the analysis of damage dynamics in wax palms. These results provide useful criteria for planning differentiated conservation measures that integrate both the spatial dimension and the individual characteristics of palm individuals.

Figure 10 presents the relationship between mean structural damage (%) in wax palms (Ceroxylon spp.) and two key ecological variables — DBH (cm) and altitude (m a.s.l.) — disaggregated by zone (AR, PR, MF, and CR) and plot (Plots 1–4) in the Molinopampa forest, Amazonas, Peru.

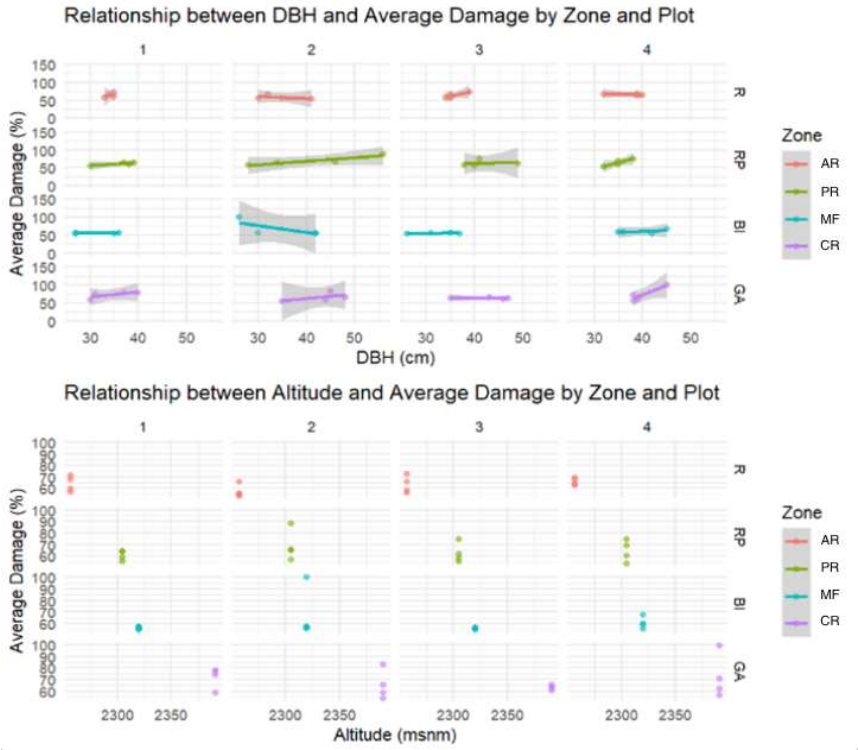

Figure 10. Relationship between DBH, Altitude and Average Damage by Zone and Plot.

In the upper panel, the relationship between DBH and damage varies by zone and plot. Overall, individuals with larger diameters tend to show higher levels of damage, particularly in zones CR and PR, suggesting that more robust palms may be more exposed to pressure factors such as pest infestation, selective extraction, or structural ageing. In the lower panel, the relationship between altitude and damage shows differentiated patterns among zones and plots. In several plots, particularly in CR and PR, a positive trend is observed, indicating that damage tends to increase with altitude. However, in zones such as MF, the relationship is more tenuous or variable, suggesting that altitude interacts with local conditions including microclimate, accessibility, and anthropogenic pressure.

Zone CR stands out for its greater dispersion and extreme values across both variables, reflecting critical deterioration hotspots. In contrast, MF maintains more homogeneous patterns and lower relative damage, though outliers reaching 100% are also present.

Collectively, these findings demonstrate that structural damage varies not only by zone and plot, but also as a function of individual structural characteristics and topographic conditions. These results provide valuable criteria for the design of differentiated conservation strategies, integrating both the protection of large-diameter palms — given their vulnerability and reproductive relevance — and adaptive management across altitudinal gradients.

 doi:10.20944/preprints202605.0217.v1

4. Discussion

The results of this study enabled the identification of internal structural variations within the stipes of Ceroxylon individuals assessed in Molinopampa Ocol, suggesting that internal damage may be influenced by anthropogenic factors. Unlike dicotyledonous trees, palms (Arecaceae) exhibit an atypical internal architecture characterized by the absence of a vascular cambium and secondary growth, in which the primary vascular tissue consists of fibrovascular bundles embedded in a ground parenchyma matrix [48–50]. This anatomical configuration produces a radially and axially heterogeneous density gradient that directly influences the propagation of elastic and electromagnetic waves [51]. According to Najmie et al. [52,53], stipe density is distributed in concentric zones, being greatest at the periphery and lowest in the medullary region, which accounts for the systematic appearance of low acoustic velocity areas in Ceroxylon tomograms.

In sonic tomography assessments, the non-homogeneous nature of the stipe and variations in parenchyma moisture content can produce signal attenuation and acoustic refraction phenomena, complicating tomogram interpretation [54,55]. Research by Lin et al. [38] and Burcham et al. [35] warns that this natural pattern of low central density increases the risk of underestimating cavities or overestimating internal degradation processes, given the reduced acoustic contrast between healthy parenchyma and tissue degraded by pathogens such as Ganoderma. As noted by Schubert et al. [56] and Carrasco et al. [57], the intrinsic anisotropy of the fibers and stem geometry are critical factors that must be rigorously calibrated in time-of-flight algorithms (such as those employed by ArborSonic 3D software) in order to accurately distinguish the structural architecture of the species from pathologies that compromise its mechanical stability.

Ceroxylon forests commonly coexist with human activities such as extensive cattle ranching [15], forest clearing for agriculture [58], selective extraction of forest resources [59], and wax production, together with religious rituals that contribute to population decline [11,20,21]. These processes generate soil compaction, habitat fragmentation, and microclimatic alterations — factors that may influence the structural dynamics of palm populations. Furthermore, active cattle presence negatively affects natural regeneration through seedling consumption, posing a significant risk to population viability. It has been estimated that, within approximately 47 years, the majority of adult individuals will disappear without sufficient seedling recruitment to ensure their replacement, thereby threatening the long-term continuity of this ecosystem [60].

The internal health status of Ceroxylon individuals reflects distinct levels of degradation associated with anthropogenic activities in the study area. Notably, elevated deterioration levels were recorded in the cattle ranching (CR) zone, where some individuals reached up to 99.25% degradation, and in the mixed forest (MF) zone, where one individual showed 100% deterioration. These conditions reflect the intensity of anthropogenic pressures, primarily linked to land-use change, agricultural expansion, and cattle ranching, which compromise natural regeneration and long-term population viability [11,20,30,60]. In this context, a loss of 2,130 ha of forest cover between 1987 and 2017 has been documented, accompanied by an increase of 2,114 ha in areas converted to pasture and cropland during the same period [30].

Despite the fact that the passive restoration (PR) and active restoration (AR) zones were considered areas with a greater degree of management and protection, both exhibited relatively high deterioration levels, with mean values of 64.0% and 62.59%, respectively. In contrast, zones subject to greater anthropogenic pressure (cattle ranching (CR) and mixed forest (MF)) recorded means of 67.9% and 59.8%, respectively. Although CR presented the highest deterioration level among all evaluated zones, MF showed the lowest mean value. This pattern suggests that the intensity of disturbance in MF was lower than that associated with post-intervention regeneration processes, in which individuals have not yet accumulated significant structural damage.

The positive correlation between DBH and mean damage suggests that larger individuals tend to exhibit greater internal deterioration, although the relationship is not particularly strong. Increases in biomass are generally associated with greater susceptibility to physical and biological stressors, as larger trees face greater physiological and biomechanical constraints that increase their vulnerability

 doi:10.20944/preprints202605.0217.v1

to environmental stress and structural failure [61]. Consequently, larger and longer-lived individuals accumulate greater exposure to fungal pathogens and mechanical damage over their lifetimes [62], which may explain the structural damage accumulation reported in Ceroxylon [63]. This pattern may be associated with both natural senescence processes and anthropogenic pressures that affect the physiological stability of palm individuals [63,64]. From an ecological standpoint, these findings highlight the importance of accounting for both individual age and size, as well as spatial variability, when planning conservation strategies, prioritizing areas with higher densities of large individuals and zones with high structural damage for management interventions [63,65].

The tomograms reveal that structural deterioration of the stipe does not follow a homogeneous distribution across the different measurement layers, exhibiting both spatial and vertical variability. The active restoration (AR) and passive restoration (PR) zones recorded damage medians of 63.38% and 62.63%, respectively, with greater dispersion in PR, where maximum values reached 88.25%. The cattle ranching (CR) zone presented a median of 64.00% and the greatest variability among all zones, with extreme values approaching 100% (99.25%). In contrast, the mixed forest (MF) zone showed the lowest median (56.38%) and a more concentrated distribution around lower damage values; however, high outliers were also recorded, reaching 100%. Collectively, these results indicate that, although MF exhibits a generally lower level of deterioration, the presence of extreme values demonstrates that damage is not entirely uniform among individuals. It is therefore possible that, even in areas with lower human impact, highly affected individuals may occur, a pattern that could be associated with cumulative degradation processes in large individuals or with selective attack by xylophagous fauna and fungi [40,66].

The detection of internal deterioration underscores the diagnostic utility of sonic tomography as a high-precision tool [67], enabling the mapping of tissue density and continuity through acoustic variations [68–70], and revealing how topographic variables and microclimates regulate the proliferation of decay agents and determine the actual exposure of palm individuals to climatic conditions [71]. Moreover, physiological stress in individual palms favors the colonization of xylophagous fungi [72], with long-term consequences for Ceroxylon populations. The structural damage detected in this study is consistent with previous assessments demonstrating the viability of sonic tomography for quantifying severe anomalies in tropical and temperate forest ecosystems [24,34,68]. However, results must be interpreted in light of the technical characteristics of the technology and the sampling design. Although the instrument is highly effective at detecting cavities and advanced damage, its precision decreases when identifying early-stage decay processes [67]. Additionally, physical properties inherent to palm tissue can affect sound propagation and must be considered when interpreting tomographic images [42]. At the experimental scale, the data obtained are valuable at the local level, but extrapolating these conclusions to the landscape scale requires assessment of larger areas. Future research should increase the number of evaluated individuals and complement sonic tomography with additional methods, such as electrical impedance tomography, which is more sensitive to moisture changes occurring in the early stages of fungal infection [73].

Internal structural deterioration in adult palms is not exclusively an indicator of poor health, but also represents a functionally important ecological process for microhabitat generation. Stipe degradation produces cavities and decay zones that serve as biologically significant structures within the ecosystem [62]. These spaces provide nesting sites, refuges, and foraging opportunities for local fauna, directly benefiting species that depend on natural cavities formed by biological decay, including birds, arboreal mammals, and invertebrates [64,74,75]. Accordingly, Ceroxylon individuals with certain levels of stipe damage may sustain networks of biotic interactions, demonstrating that palms exhibiting mechanical damage are important for maintaining ecosystem biodiversity levels [76]. Conservation and management strategies must therefore also ensure the protection of areas containing senescent or internally decayed palms, recognizing these individuals as key structural elements for maintaining the high diversity of the ecosystem [77].

The integration of topographic and climatic data at the local scale will enable the design of more effective mitigation strategies [78], aimed not only at biodiversity conservation but also at

 doi:10.20944/preprints202605.0217.v1

strengthening ecosystem climate resilience [79,80] and ensuring the continuity of ecosystem services [81], including hydrological regulation and carbon sequestration [82,83]. In this context, ensuring legal protection against deforestation and guaranteeing the structural stability of remnant individuals are essential for the targeted and sustainable conservation of montane forest functionality [82]. Furthermore, the combination of non-invasive techniques and statistical analyses enables the identification of vulnerability patterns and supports evidence-based conservation decision-making, contributing to the preservation of ecological function and associated ecosystem services [24,84].

In particular, the identification of zones exhibiting greater structural deterioration, especially the cattle ranching (CR) areas, enables the prioritization of sectors for monitoring and management, strengthening strategies aimed at maintaining the population stability of Ceroxylon in Andean montane forests. Within this framework, the implementation of effective legal protection mechanisms, both in privately managed territories (Private Conservation Areas, PCAs) and in those under state administration (Natural Protected Areas, NPAs), is essential for safeguarding these ecological functions. Effective management of such areas not only ensures ecosystem resilience, but constitutes a global priority in the face of the current climate and biodiversity crisis [79,80].

5. Conclusions

This study demonstrates that the internal structural integrity of Ceroxylon palms in the tropical montane forests of the Peruvian Andes is significantly compromised, with mean structural deterioration reaching 63.58% across all evaluated zones. The findings reveal that anthropogenic land-use histories directly influence forest health, as evidenced by the significantly higher and more variable damage levels recorded in the cattle ranching (CR) zone compared to the mixed forest (MF) zone, which served as a less disturbed reference site. Furthermore, the significant positive correlation between diameter at breast height (DBH) and mean structural damage suggests that larger, mature individuals accumulate greater internal decay over time, potentially due to prolonged exposure to environmental stressors and biological pathogens — including xylophagous fungi. While altitude showed no significant association with phytosanitary condition, the high levels of internal degradation detected — frequently invisible upon external inspection — confirm that sonic tomography constitutes a highly effective, non-invasive diagnostic tool for monitoring the structural stability of Andean palm populations. Collectively, these results underscore the urgent need for differentiated conservation strategies that prioritize the protection of large-diameter individuals, the mitigation of cattle grazing pressures, and the implementation of effective legal protection mechanisms within both Private Conservation Areas (PCAs) and Natural Protected Areas (NPAs), in order to ensure the long-term population viability and ecosystem functionality of Ceroxylon forests in the tropical Andes.

Author Contributions: Conceptualization, D.G.-T., A.S.-I. and F.C.-G.; methodology, Y.Q.-G., J.M.-B. and D.G.-T; software, Y.Q.-G.; validation, A.S.-I. and F.C.-G.; formal analysis, Y.Q.-G. and J.M.-B.; investigation, Y.Q.-G., M.C.-B., B.P.-T. and D.G.-T.; resources, A.S.-I. and M.L.R.-S.; data curation, M.L.R.-S. and P.M.-I.; writing—original draft preparation, Y.Q.-G. and M.C.-B.; writing—review and editing, A.S.-I., F.C.-G., J.M.-B., M.L.R.-S., F.A.-A. and L.A.L.-B.; visualization, Y.Q.-G.; supervision, A.S.-I., F.C.-G. and M.L.R.-S.; project administration, A.S.-I.; funding acquisition, A.S.-I. and M.L.R.-S. All authors have read and agreed to the published version of the manuscript.

Funding: This research was supported by the Universidad Nacional Mayor de San Marcos through the PSINFINV Project entitled "Tomografía Sónica y estado de conservación de especies clave en relictos de vegetación y áreas de conservación en territorios andino-amazónicos del Perú", Project Code No. B24140332 (RR No. 015116-2024-R/UNMSM).

Data Availability Statement: Data used in this study can be requested from the corresponding author via email: abel.salinas1@unmsm.edu.pe.

Conflicts of Interest: The authors declare no conflicts of interest.

 doi:10.20944/preprints202605.0217.v1

References

1. Baker, W.J.; Dransfield, J. Beyond Genera Palmarum: Progress and prospects in palm systematics. *Bot. J. Linn. Soc.* **2016**, *182*, 207–233. https://doi.org/10.1111/boj.12401
2. Pintaud, J.C.; Galeano, G.; Balslev, H.; Bernal, R.; Borchsenius, F.; Ferreira, E.; de Granville, J.J.; Mejía, K.; Millán, B.; Moraes, M.; et al. Las palmeras de América del Sur: Diversidad, distribución e historia evolutiva. *Rev. Peru. Biol.* **2008**, *15*, 7–29.
3. Quinteros-Gómez, Y.; Zarco-González, M.; Ticerán, D.; Agramont, A.; Monroy-Vilchis, O. Effects of human disturbance on above-ground carbon stocks in north-west Amazonian *Mauritia flexuosa* peat swamp forests. *Mires Peat* **2023**, *29*, 5. https://doi.org/10.19189/MaP.2021.OMB.StA.2300
4. Muscarella, R.; Emilio, T.; Phillips, O.L.; Lewis, S.L.; Slik, F.; Baker, W.J.; Couvreur, T.L.P.; Eiserhardt, W.L.; Svenning, J.C.; Affum-Baffoe, K.; et al. The global abundance of tree palms. *Glob. Ecol. Biogeogr.* **2020**, *29*, 1495–1514. https://doi.org/10.1111/geb.13123
5. Dransfield, J.; Uhl, N.W.; Asmussen, C.B.; Baker, W.J.; Harley, M.M.; Lewis, C.E. *Genera Palmarum: The Evolution and Classification of Palms*; Kew Publishing: Richmond, UK, 2008.
6. Eiserhardt, W.L.; Svenning, J.C.; Kissling, W.D.; Balslev, H. Geographical ecology of the palms (Arecaceae): Determinants of diversity and distributions across spatial scales. *Ann. Bot.* **2011**, *108*, 1391–1416. https://doi.org/10.1093/aob/mcr146
7. Henderson, A. *Evolution and Ecology of Palms*; New York Botanical Garden Press: New York, NY, USA, 2002.
8. Zona, S.; Henderson, A. A review of animal-mediated seed dispersal of palms. *Selbyana* **1989**, *11*, 6–21.
9. Agostini-Costa, T.S. Bioactive compounds and health benefits of some palm species traditionally used in Africa and the Americas - A review. *J. Ethnopharmacol.* **2018**, *224*, 202–229. https://doi.org/10.1016/j.jep.2018.05.035
10. Quinteros-Gómez, Y.M.; Monroy-Vilchis, O.; Zarco-González, M.M.; Endara-Agramont, A.R.; Pacheco, X.P. Floristic composition, structure and species conservation status of *Mauritia flexuosa* palm swamps in Andean-Amazonian piedmont in the Department of San Martín, Peru. *Rev. Mex. Biodivers.* **2021**, *92*, e923186. https://doi.org/10.22201/ib.20078706e.2021.92.3186
11. Sanín, M.J.; Galeano, G. A revision of the Andean wax palms, *Ceroxylon* (Arecaceae). *Phytotaxa* **2011**, *34*, 1–64. https://doi.org/10.11646/phytotaxa.34.1.1
12. Valdivia, M.I.V.; Gamarra, L.V. A new species of *Ceroxylon* (Arecaceae) from Cordillera Azul National Park—Peru. *Phytotaxa* **2021**, *483*, 267–276. https://doi.org/10.11646/phytotaxa.483.3.6
13. Santa Cruz, L.; Pintaud, J.-C.; Rojas-Fox, V.; Ramírez, R.; Rodríguez Rodríguez, E.F. Inventario de las palmeras de la vertiente occidental del Perú. *Arnaldoa* **2018**, *25*, 857–876. https://doi.org/10.22497/arnaldoa.253.25304
14. Suárez, D.; Mejía, A.; Marín, O.; Agudelo, L.D. Proposal for nutritional management in Palma of cera (*Ceroxylon quindiuense* wendl.) low growth condition in vehicular high flow vehicle mesh. *J. Res. Eng. Sci.* **2016**, *1*, 163. https://doi.org/10.33133/jres-1-2016-163
15. Benítez, Á.; Ramón, P.; Sarango, M.; Torracchi-Carrasco, E. Spatial patterns of *Ceroxylon parvifrons* (Engel) H. Wendl of the montane forests in Southern Ecuador. *Int. J. For. Res.* **2022**, *2022*, 5707906. https://doi.org/10.1155/2022/5707906
16. Huisman, S.N.; Raczka, M.F.; McMichael, C.N.H. Palm phytoliths of mid-elevation Andean forests. *Front. Ecol. Evol.* **2018**, *6*, 193. https://doi.org/10.3389/fevo.2018.00193
17. Sanín, M.J.; Kissling, W.D.; Bacon, C.D.; Borchsenius, F.; Galeano, G.; Svenning, J.C.; de Granville, J.J.; Mejía, K.; Pintaud, J.C. The Neogene rise of the tropical Andes facilitated diversification of wax palms (*Ceroxylon*: Arecaceae) through geographical colonization and climatic niche separation. *Bot. J. Linn. Soc.* **2016**, *182*, 303–317. https://doi.org/10.1111/boj.12419
18. Montúfar, R.; Anthelme, F.; Pintaud, J.C.; Balslev, H. Disturbance and resilience in tropical American palm populations and communities. *Bot. Rev.* **2011**, *77*, 426–461. https://doi.org/10.1007/s12229-011-9085-9
19. Galeano, G.; Bernal, R. Palmas (familia Arecaceae o Palmae). In *Libro Rojo de Plantas de Colombia*; Calderón, E., Galeano, G., García, N., Eds.; Instituto de Ciencias Naturales-Universidad Nacional de Colombia: Bogotá, Colombia, 2005; Volume 2, pp. 59–224.

 doi:10.20944/preprints202605.0217.v1

20. Anthelme, F.; Lincango, J.; Gully, C.; Duarte, N.; Montúfar, R. How anthropogenic disturbances affect the resilience of a keystone palm tree in the threatened Andean cloud forest? *Biol. Conserv.* **2011**, *144*, 1059–1067. https://doi.org/10.1016/j.biocon.2011.01.002
21. Balslev, H.; Copete, J.C.; Pedersen, D.; Bernal, R.; Galeano, G.; Duque, Á.; Sanín, M.J. Palm diversity and abundance in the Colombian Amazon. In *Forest Structure, Function and Dynamics in Western Amazonia*; Mistretta, P., Ed.; Wiley-Blackwell: Hoboken, NJ, USA, 2015; pp. 101–123.
22. Barmpoutis, P.; Papaioannou, P.; Dimitropoulos, K.; Grammalidis, N. A Review on Early Forest Fire Detection Systems Using Optical Remote Sensing. *Sensors* **2020**, *20*, 6442. https://doi.org/10.3390/s20226442
23. Gao, B.; Jia, W.; Wang, Q.; Yang, G. All-weather forest fire automatic monitoring and early warning application based on multi-source remote sensing data: Case study of Yunnan. *Fire* **2025**, *8*, 344. https://doi.org/10.3390/fire8090344
24. Quinteros-Gómez, Y.; Salinas-Inga, A.; Macedo-Bedoya, J.; Peralta-Alcantara, E.; La Rosa-Sánchez, M.; Camones-Gonzales, F.; Yamunaque, A.; Angeles-Alvarez, F.; Gómez-Ticerán, D.; Solano-Dávila, O.L. Noninvasive sonic tomography for the detection of internal defects in relict woodlands of *Polylepis* in Peru. *Forests* **2025**, *16*, 957. https://doi.org/10.3390/f16060957
25. Kurbanov, E.; Vorobev, O.; Lezhnin, S.; Sha, J.; Wang, J.; Li, X.; Cole, J.; Dergunov, D.; Wang, Y. Remote sensing of forest burnt area, burn severity, and post-fire recovery: A review. *Remote Sens.* **2022**, *14*, 4714. https://doi.org/10.3390/rs14194714
26. Vasilakos, C.; Tsekouras, G.E.; Kavroudakis, D. LSTM-based prediction of Mediterranean vegetation dynamics using NDVI time-series data. *Land* **2022**, *11*, 923. https://doi.org/10.3390/land11060923
27. Adão, T.; Hruška, J.; Pádua, L.; Bessa, J.; Peres, E.; Morais, R.; Sousa, J.J. Hyperspectral imaging: A review on UAV-based sensors, data processing and applications for agriculture and forestry. *Remote Sens.* **2017**, *9*, 1110. https://doi.org/10.3390/rs9111110
28. Liu, J.; Feng, Z.; Mannan, A.; Khan, T.U.; Cheng, Z. Comparing non-destructive methods to estimate volume of three tree taxa in Beijing, China. *Forests* **2019**, *10*, 92. https://doi.org/10.3390/f10020092
29. Lee, B.J.; Son, S.; Jung, J.K.; Park, Y. Non-invasive assessment of the internal condition of urban trees infested by two cerambycid beetles, *Aromia bungii* and *Massicus raddei*, using sonic tomography. *Forests* **2024**, *15*, 1231. https://doi.org/10.3390/f15071231
30. Montoya-Rojas, R. Análisis multitemporal de cambio de uso del suelo y cobertura vegetal en el área de conservación privada bosques de palmera, Ocol - Amazonas, período 1987-2017. Undergraduate Thesis, Universidad Nacional Toribio Rodríguez de Mendoza de Amazonas, Chachapoyas, Peru, 2020.
31. Bruijnzeel, L.A.; Scatena, F.N.; Hamilton, L.S. *Tropical Montane Cloud Forests: Science for Conservation and Management*; Cambridge University Press: Cambridge, UK, 2011.
32. Galeano, G.; Bernal, R. *Palms of the Americas*; Princeton University Press: Princeton, NJ, USA, 2010.
33. [Falta referencia: Luis et al., 2020]
34. Young, K.R.; León, B. Peru's Humid Eastern Montane Forests: An Overview of Their Physical Settings, Biological Diversity, Human Use and Settlement, and Conservation Needs; DIVA Technical Report 5; Centre for Research on the Cultural and Biological Diversity of Andean Rainforests (DIVA): Rønde, Denmark, 1999.
35. Burcham, D.C.; Brazee, N.J.; Marra, R.E.; Kane, B. Geometry matters for sonic tomography of trees. *Trees* **2023**, *37*, 335–347. https://doi.org/10.1007/s00468-023-02387-4
36. Ross, R.J. *Nondestructive Evaluation of Wood: Second Edition*; General Technical Report FPL-GTR-238; USDA Forest Service, Forest Products Laboratory: Madison, WI, USA, 2015.
37. Gilbert, E.A.; Smiley, E.T. Picus sonic tomography for the quantification of decay in white oak (*Quercus alba*) and hickory (*Carya* spp.). *J. Arboric.* **2004**, *30*, 277–281. https://doi.org/10.48044/jauf.2004.033
38. Lin, C.J.; Chang, T.T.; Juan, M.Y. Detecting deterioration in royal palm (*Roystonea regia*) using ultrasonic tomographic and resistance microdrilling techniques. *J. Trop. For. Sci.* **2011**, *23*, 37–45.
39. Wang, X. Acoustic measurements on trees and logs: A review and analysis. *Wood Sci. Technol.* **2013**, *47*, 965–975. https://doi.org/10.1007/s00226-013-0552-9
40. Gilbert, G.S.; Ballesteros, J.O.; Barrios-Rodriguez, C.A.; Bonadies, E.F.; Cedeño-Sánchez, M.L.; Fossatti-Caballero, N.J.; Trejos-Rodríguez, M.M.; Pérez-Suñiga, J.M.; Holub-Young, K.S.; Henn, L.A.W.; et al. Use

 doi:10.20944/preprints202605.0217.v1

of sonic tomography to detect and quantify wood decay in living trees. *Appl. Plant Sci.* **2016**, *4*, 1600060. https://doi.org/10.3732/apps.1600060

41. Divos, F.; Divos, P. Resolution of stress wave based acoustic tomography. In Proceedings of the 14th International Symposium on Nondestructive Testing of Wood, Hannover, Germany, 28–30 September 2005; pp. 309–314.
42. Wang, X.; Allison, R.B. Decay detection in red oak trees using a combination of visual inspection, acoustic testing, and resistance microdrilling. *Arboric. Urban For.* **2008**, *34*, 1–4. https://doi.org/10.48044/jauf.2008.001
43. Helmanto, H.; Kristiati, E.; Wardhani, F.F.; Zulkarnaen, R.N.; Sahromi; Mujahidin; Rachmadiyanto, A.N.; Abdurachman. Tree health assessment of *Agathis borneensis* Warb. in Bogor Botanical Garden using arborsonic. *IOP Conf. Ser. Earth Environ. Sci.* **2018**, *203*, 012032. https://doi.org/10.1088/1755-1315/203/1/012032
44. Bates, D.; Mächler, M.; Bolker, B.; Walker, S. Fitting Linear Mixed-Effects Models Using lme4. *J. Stat. Softw.* **2015**, *67*, 1–48. https://doi.org/10.18637/jss.v067.i01
45. Wickham, H. *ggplot2: Elegant Graphics for Data Analysis*; Springer: New York, NY, USA, 2016; ISBN 978-3-319-24277-4.
46. Wickham, H.; François, R.; Henry, L.; Müller, K.; Vaughan, D. *dplyr: A Grammar of Data Manipulation*, R package version 1.1.4; 2023. Available online: https://CRAN.R-project.org/package=dplyr
47. Kuznetsova, A.; Brockhoff, P.B.; Christensen, R.H.B. lmerTest Package: Tests in Linear Mixed Effects Models. *J. Stat. Softw.* **2017**, *84*, 1–26. https://doi.org/10.18637/jss.v084.i13
48. Tomlinson, P.B.; Horn, J.W.; Fisher, J.B. *The Anatomy of Palms: Arecaceae—Palmae*; Oxford University Press: Oxford, UK, 2011.
49. Parthsarathy, M.V.; Klotz, L.H. Palm wood I. Anatomical aspects. *Wood Sci. Technol.* **1976**, *10*, 215–229. https://doi.org/10.1007/BF00355742
50. Sainz-Resendiz, B.A.; Estrada-Ruiz, E.; Mateo-Cid, L.E.; Porras-Múzquiz, H. Primer registro de un estípite de Coryphoideae: *Palmoxylon kikaapoa* de la Formación Olmos del Cretácico Superior, Coahuila, México. *Rev. Mex. Biodivers.* **2015**, *86*, 872–881. https://doi.org/10.1016/j.rmb.2015.09.009
51. Zimmermann, M.H.; Tomlinson, P.B. Analysis of the complex vascular system of palms: Arecaceae. *Science* **1966**, *152*, 72–73. https://doi.org/10.1126/science.152.3718.72
52. Najmie, M.; Khalid, K.; Aziz, S.; Jusoh, A. Density and ultrasonic characterization of oil palm trunk infected by *Ganoderma* boninense disease. Meas. Sci. Rev. 2011, 11, 160–164. https://doi.org/10.2478/v10048-011-0026-x
53. Taban, E., Khavanin, A., Ohadi, A., Putra, A., Jafari, A., Faridan, M., & Soleimanian, A. (2019). Study on the acoustic characteristics of natural date palm fibres: Experimental and theoretical approaches. Building and Environment. https://doi.org/10.1016/j.buildenv.2019.106274.
54. Smiley ET, Matheny N, Lilly S. Best management practices: tree risk assessment. Champaign (IL): International Society of Arboriculture; **2011**.
55. Costa, M.W.; et al. Detection of internal decay in palm trees using sonic tomography. *Arboric. Urban For.* **2019**, *45*, 110–122.
56. Schubert, S.; Gsell, D.; Dual, J.; Motavalli, M.; Niemz, P. Acoustic wood tomography on trees and the challenge of wood heterogeneity. *Holzforschung* **2009**, *63*, 107–112. https://doi.org/10.1515/HF.2009.028
57. Alves RC, Mantilla JN, Bremer CF, Carrasco EV. Application of acoustic tomography and ultrasonic waves to estimate stiffness constants of muiracatiara Brazilian wood. *BioResources*. 2015;10(1):1845–56.
58. Anthelme F, Lincango J, Gully C, Duarte N, Montúfar R. How anthropogenic disturbances affect the resilience of a keystone palm tree in the threatened Andean cloud forest? *Forests*. 2022;13(3):1–14
59. Agualzaca Caisaguano, D.O.; Llumitasig Quinatoa, M.S.; Cusquillo Quispillo, B.D.; Carranza Patiño, M.; Jiménez Romero, E.M. Propuesta de plan de manejo integral para *Ceroxylon echinulatum* basado en criterios ecológicos en la comunidad Mocata, Pallatanga (Ecuador). *Multidiscip. Collab. J.* **2025**, *3*, 227–245. https://doi.org/10.70881/mcj/v3/n2/63
60. Bernal, R.; Sanín, M.J. The palm stands of *Ceroxylon quindiuense* (Arecaceae) in the Cocora Valley, Quindío: Perspectives on an iconic Colombian landscape. *Colomb. For.* **2013**, *16*, 67–79. https://doi.org/10.14483/udistrital.jour.colomb.for.2013.1.a05

 doi:10.20944/preprints202605.0217.v1

61. Bennett, A.C.; McDowell, N.G.; Allen, C.D.; Anderson-Teixeira, K.J. Larger trees suffer most during drought in forests worldwide. *Nat. Plants* **2015**, *1*, 15139. https://doi.org/10.1038/nplants.2015.139
62. Lindenmayer, D.B.; Laurance, W.F.; Franklin, J.F. Global decline in large old trees. *Science* **2012**, *338*, 1305–1306. https://doi.org/10.1126/science.1231070
63. Sanín, M.J.; Anthelme, F.; Pintaud, J.C.; Galeano, G.; Bernal, R. Juvenile resilience and adult longevity explain residual populations of the Andean wax palm *Ceroxylon quindiuense* after deforestation. *PLoS ONE* **2013**, *8*, e74139. https://doi.org/10.1371/journal.pone.0074139
64. Chacón-Vargas, K.; García-Merchán, V.H.; Sanín, M.J. From keystone species to conservation: Conservation genetics of wax palm *Ceroxylon quindiuense* in the largest wild populations of Colombia and selected neighboring ex situ plant collections. *Biodivers. Conserv.* **2020**, *29*, 283–302. https://doi.org/10.1007/s10531-019-01882-w
65. Kozák, D.; Svitok, M.; Zemlerová, V.; Mikoláš, M.; Lachat, T.; Larrieu, L.; Paillet, Y.; Buechling, A.; Bače, R.; Keeton, W.S.; et al. Importance of conserving large and old trees to continuity of tree-related microhabitats. *Conserv. Biol.* **2023**, *37*, e14066. https://doi.org/10.1111/cobi.14066
66. Gilbert, G.S.; Faircloth, B.C.; Glenn, T.C.; Ballesteros, J.O.; Barrios-Rodríguez, C.A.; Bonadies, E.; Cedeño-Sánchez, M.L.; Fossatti-Caballero, N.J.; Pérez-Suñiga, J.M.; Trejos-Rodríguez, M.M.; et al. Hidden decay of live trees in a tropical rain forest. *Ecology* **2025**, *106*, e70208. https://doi.org/10.1002/ecy.70208
67. Deflorio, G.; Fink, S.; Schwarze, F.W.M.R. Detection of incipient decay in tree stems with sonic tomography after wounding and fungal inoculation. *Wood Sci. Technol.* **2008**, *42*, 117–132. https://doi.org/10.1007/s00226-007-0159-0
68. Li, P.; Feng, H.; Zhang, H.; Wang, X. Evaluation of internal decay in standing trees using sonic tomography and stress wave techniques. *Sensors* **2020**, *20*, 695. https://doi.org/10.3390/s20030695
69. Wang, X.; Allison, R.B.; Wang, L.; Ross, R.J. *Acoustic Tomography for Decay Detection in Red Oak Trees*; Research Paper FPL-RP-642; USDA Forest Service, Forest Products Laboratory: Madison, WI, USA, 2004.
70. Bucur, V. *Acoustics of Wood*, 2nd ed.; Springer: Berlin/Heidelberg, Germany, 2006. https://doi.org/10.1007/3-540-30594-7
71. Zellweger, F.; De Frenne, P.; Lenoir, J.; Vangansbeke, P.; Verheyen, K.; Bernhardt-Römermann, M.; Baeten, L.; Hédl, R.; et al. Forest microclimate dynamics drive plant responses to warming. *Science* **2020**, *368*, 772–775. https://doi.org/10.1126/science.aba6880
72. Saine, S.; Penttilä, R.; Fukami, T.; Furneaux, B.; Hytönen, T.; Miettinen, O.; Monkhouse, N.; et al. Idiosyncratic responses to biotic and environmental filters in wood-inhabiting fungal communities. *Ecology* **2025**, *106*, e70013. https://doi.org/10.1002/ecy.70013
73. Brazee, N.J.; Marra, R.E.; Göcke, L.; Van Wassenaer, P. Non-destructive assessment of internal decay in three hardwood species of northeastern North America using sonic and electrical impedance tomography. *Forestry* **2011**, *84*, 33–39. https://doi.org/10.1093/forestry/cpq040
74. Renton, K.; Salinas-Melgoza, A.; De Labra-Hernández, M.A.; de la Parra-Martínez, S.M. Resource requirements of parrots: Nest site selectivity and dietary plasticity of Psittaciformes. *J. Ornithol.* **2015**, *156*, 73–90. https://doi.org/10.1007/s10336-015-1255-9
75. Molina, D. Secularise to conserve: The history of the wax palm in Colombia. *Plant Perspect.* **2024**, *1*, 1–25. https://doi.org/10.3197/whppp.63845494909745
76. Lindenmayer, D.B.; Laurance, W.F. The ecology, distribution, conservation and management of large old trees. *Biol. Rev.* **2017**, *92*, 1434–1458. https://doi.org/10.1111/brv.12290
77. Jones, C.G.; Lawton, J.H.; Shachak, M. Organisms as ecosystem engineers. *Oikos* **1994**, *69*, 373–386. https://doi.org/10.2307/3545850
78. De Frenne, P.; Zellweger, F.; Rodríguez-Sánchez, F.; Scheffers, B.R.; Hylander, K.; Luoto, M.; Fauset, S.; Verheyen, K.; Lenoir, J. Forest microclimates and climate change: Importance, drivers and future perspectives. *Glob. Chang. Biol.* **2021**, *27*, 2279–2297. https://doi.org/10.1111/gcb.15569
79. Lovejoy, T.E.; Nobre, C. Amazon tipping point. *Sci. Adv.* **2018**, *4*, eaat2340. https://doi.org/10.1126/sciadv.aat2340

 doi:10.20944/preprints202605.0217.v1

80. Seddon, N.; Smith, A.; Smith, P.; Key, I.; Chausson, A.; Girardin, C.; Cassidy, M.; Turner, B. Getting the message right on nature-based solutions to climate change. *Glob. Chang. Biol.* **2021**, *27*, 1518–1546. https://doi.org/10.1111/gcb.15513
81. Watson, J.E.M.; Evans, T.; Venter, O.; Williams, B.; Tulloch, A.; Stewart, C.; Thompson, I.; Ray, J.C.; Murray, K.; Salazar, A.; et al. The exceptional value of intact forest ecosystems. *Nat. Ecol. Evol.* **2018**, *2*, 599–610. https://doi.org/10.1038/s41559-018-0490-x
82. Griscom, B.W.; Adams, J.; Ellis, P.W.; Houghton, R.A.; Lomax, G.; Miteva, D.A.; Schlesinger, W.H.; Shoch, D.; Siikamäki, J.V.; Smith, P.; et al. Natural climate solutions. *Proc. Natl. Acad. Sci. USA* **2017**, *114*, 11645–11650. https://doi.org/10.1073/pnas.1710465114
83. Pan, Y.; Birdsey, R.A.; Fang, J.; Houghton, R.; Kauppi, P.E.; Kurz, W.A.; Phillips, O.L.; Shvidenko, A.; Lewis, S.L.; Canadell, J.G.; et al. A large and persistent carbon sink in the world's forests. *Science* **2011**, *333*, 988–993. https://doi.org/10.1126/science.1201609
84. Durlak, W.; Dudkiewicz-Pietrzyk, M.; Szot, P. Historic trees, modern tools: Innovative health assessment of a linden avenue in an urban environment. *Sustainability* **2025**, *17*, 9681. https://doi.org/10.3390/su17219681